

Regional Gene Expression Profile Comparison Reveals the Unique Transcriptome of the Optic Fissure

Mingzhe Cao,¹ Jiamin Ouyang,¹ Huilin Liang,¹ Jingyi Guo,¹ Siyuan Lin,¹ Shulan Yang,² Ting Xie,³ and Shuyi Chen^{1,4}

¹State Key Laboratory of Ophthalmology, Zhongshan Ophthalmic Center, Sun Yat-sen University, Guangzhou, China

²Translational Medicine Centre, The First Affiliated Hospital, Sun Yat-sen University, Guangzhou, China

³Stowers Institute for Medical Research, Kansas City, Missouri, United States

⁴Guangdong Province Key Laboratory of Brain Function and Disease, Zhongshan School of Medicine, Sun Yat-sen University, Guangzhou, China

Correspondence: Shuyi Chen, State Key Laboratory of Ophthalmology, Zhongshan Ophthalmic Center, Sun Yat-sen University, 54 South Xianlie Road, Guangzhou 510060, China; chenshy23@mail.sysu.edu.cn.

MC and JO contributed equally to the work presented here and should therefore be regarded as equivalent authors.

Submitted: January 27, 2018

Accepted: October 29, 2018

Citation: Cao M, Ouyang J, Liang H, et al. Regional gene expression profile comparison reveals the unique transcriptome of the optic fissure. *Invest Ophthalmol Vis Sci.* 2018;59:5773-5784. <https://doi.org/10.1167/iovs.18-23962>

PURPOSE. The optic fissure (OF) is a transient opening in the ventral optic cup (OC) that acts as a passage for blood vessels and retinal ganglion cell axons during early eye development. Failure to close the OF is the developmental basis for uveal coloboma, a congenital blinding eye disease that significantly contributes to childhood blindness. Genes specifically expressed in the OF region may play important roles in OF development and function. The aim of this study was to characterize the transcriptome of OC cells in the OF region and investigate the function of OF-specific genes during OF closure.

METHODS. Laser-assisted microdissection was used to collect different regions of OC tissues. Microarray analysis was used to obtain and compare gene expression profiles of different OC regions. RNA in situ hybridization (ISH) was used to further characterize OF-specific gene expression patterns. Morpholino knockdown in zebrafish was used to study the function of a newly discovered OF-specific gene during OF closure.

RESULTS. Microarray comparison revealed that the OC at the OF region exhibited a unique gene expression profile. OC expression patterns of a number of newly discovered OF-specific genes were confirmed by ISH. Morpholino knockdown and downstream target expression and function analysis demonstrated that *afap112*, a newly discovered OF-specific gene, controls OF closure by regulating *pax2a* expression.

CONCLUSIONS. Our study characterized the unique transcriptome of the OF region of the OC and demonstrated the essential role of a newly discovered OF-specific gene in OF closure. This study provides a valuable foundation for future mechanism dissection in OF development and physiology, and for human coloboma etiology exploration.

Keywords: optic fissure, coloboma, transcriptome, *Afap112*

The optic fissure (OF) is a transient opening on the ventral side of the developing retina that closes at the end of the retina morphogenesis process. Failure to close the OF is the developmental basis for uveal coloboma, a sight-threatening congenital eye malformation manifested as the absence of tissues in the inferonasal region of the retina, iris, ciliary body, choroid, and/or optic nerve.¹ It is reported that uveal coloboma affects 0.5 to 2.6 people per 10,000 births, depending on the studied population.² Uveal coloboma can occur as an isolated disease or as a symptom in systemic syndromes. Risk factors during pregnancy, such as vitamin A deficiency, alcohol exposure, or diabetes, may contribute to coloboma formation^{1,3}; however, a large proportion of coloboma cases appear to be genetic in origin.^{1,2} Ophthalmic genetic studies have linked many genes with coloboma, such as *ZEB2*, *PITX3*, *FBN2*, *SHH*, *PAX6*, *PAX2*, *CHD7*, *ABCB6*, and *SALL2*; however, the genetic causes of most coloboma cases are unclear,^{1,2,4-7} partially due to the complexity of the regulatory mechanisms involved in OF morphogenesis processes.^{1,8,9}

Vertebrate retina morphogenesis begins when the neural tube at the forebrain region protrudes bilaterally to form the

optic vesicle, which then invaginates to form the optic cup (OC). The OC is composed of the single-cell-layered retinal pigmented epithelium (RPE) and the pseudo-stratified neural retina. During the OC invagination period, a groove forms on the ventral side of the OC, extending from the distal edge of the retina to the proximal end of the optic stalk (OS), and is termed the OF. During early retina development, the OF provides the pathway for axons of newly generated retinal ganglion cells to project out of retina and for periocular mesenchymal (POM) cells to migrate into the retina, which give rise to hyaloid vessels to supply nutrients to the developing retina.¹⁰ Later, the OF gradually closes during development to seal the ventral OC, leaving only one opening at the center of the OC, the optic disc, that allows retinal ganglion cell axons to exit and blood vessels to enter the eye^{8,9} (Fig. 1A). Thus, both formation and closure of the OF are important morphogenetic events during eye development.

Animal model studies have linked several cellular events with OF development and closure. For example, because the OF is a ventral retina-specific structure, OF development is tightly linked with ventral retina development.¹¹ Accordingly,



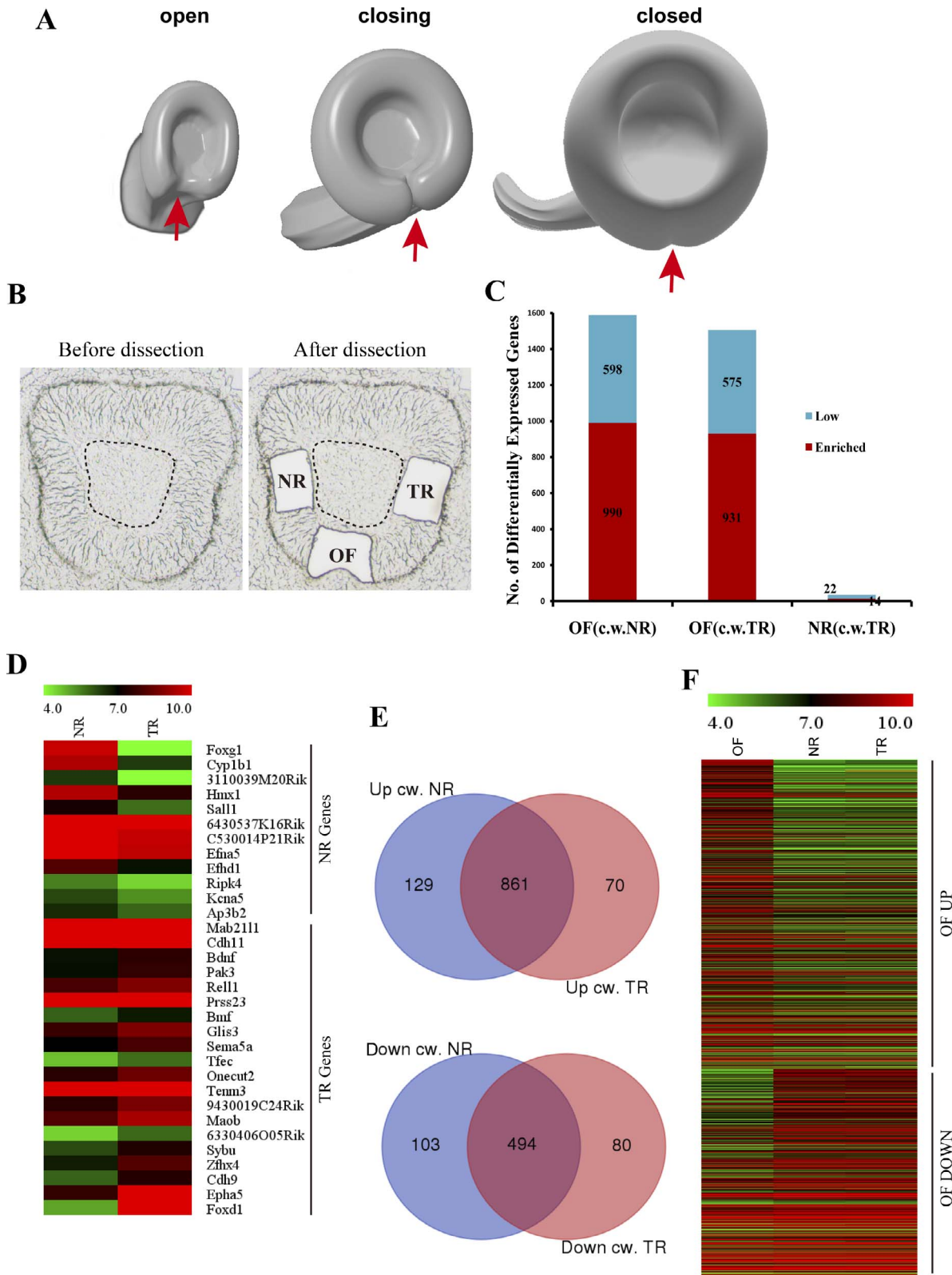


FIGURE 1. The OF expresses a unique transcriptome. **(A)** Diagrams illustrating OF morphogenesis. *Red arrows* point to the OF **(B)** Brightfield images of an OC before and after microdissection. **(C)** The chart summarizes the number of differentially expressed genes (DEGs) in the OF, NR, and TR (c.w.: compared with). **(D)** The heatmap of DEGs between the NR and TR. **(E)** Venn diagrams showing the number of genes shared by lists of DEGs between the OF-NR and OF-TR comparisons. **(F)** Heatmap of DEGs between the OF and NR/TR.

mutations affecting ventral retina fate determination, such as mutations in *Vax1* and *Vax2*, lead to coloboma formation.¹²⁻¹⁴ Similarly, OF development is also closely related to the retinal proximal structure, the OS, which connects the retina to the central brain. Genes regulating the retinal proximal fates often play important roles in OF development. For example, OS fate regulator *Pax2* and body midline sonic hedgehog (SHH) signaling are both essential in OF development and closure.¹⁴⁻¹⁶ In addition to optic tissues, surrounding POM cells also support OF development; when the POM does not develop well, OF closure is often affected.¹⁷⁻²⁰ Cell proliferation provides forces to drive tissue expansion and movement and thus is often involved in morphogenesis processes during development. Studies have shown that retinal progenitor cell proliferation needs to be tightly controlled for successful OF closure.²¹ Similarly, cell-cell and cell-extracellular matrix interactions are essential for tissue morphogenesis and need to be tightly controlled and actively adjusted for OF closure to proceed successfully. Mutations in adhesion molecules and cytoskeleton regulators have been found to contribute to coloboma formation.^{22,23}

We reason that the OC cells surrounding the OF are the cells that directly participate in the OF fusion process; many known key OF regulatory genes are specifically expressed in the region. Characterizing the transcriptome of these cells may provide valuable information on the regulatory mechanisms governing OF closure. In this study, we used laser-assisted microdissection to collect OC cells in different areas of the OC, including the OF region, and used microarrays to compare the transcriptomes of different regions. Subsequent gene knock-down studies in zebrafish demonstrated that *afap112*, the gene most highly enriched in the OF transcriptome revealed by microarray analysis, partially controls OF closure by regulating *pax2a* expression. Thus, our study revealed the unique gene expression profile of OC cells in the OF region, and indicates that the newly discovered OF-specific genes may play important roles in OF development.

MATERIALS AND METHODS

Animal Maintenance

All animal studies were performed in compliance with the ARVO Statement for the Use of Animals in Ophthalmic and Vision Research and were approved by the Institutional Animal Care and Use Committee of Zhongshan Ophthalmic Center. Wild-type C57BL/6J male and female mice were caged together in the afternoon, and vaginal plugs were checked the next morning to obtain time-matched embryos. Noon on the day that a vaginal plug was found was counted as embryonic day 0.5 (E0.5). Wild-type AB zebrafish embryos were obtained through natural spawning, raised at 28.5°C, and staged in hours post fertilization (hpf). Zebrafish embryos were treated with 0.003% phenylthiourea (Sigma-Aldrich Corp., St. Louis, MO, USA) starting from 20 hpf to prevent pigmentation when necessary.

Laser-Assisted Microdissection, Microarray Analysis, and Quantitative RT-PCR

Immediately after euthanization, heads of embryonic day 11.5 (E11.5) wild-type C57BL/6J mice were embedded in OCT tissue freezing medium (Leica, Wetzlar, Germany) in a sagittal orientation and frozen. Mouse embryonic head blocks were sectioned and mounted onto glass slides using a cryostat microtome (Leica CM 1950). Sections were fixed briefly in 75% ethanol for 2 minutes, stained with hematoxylin for 2 minutes,

dehydrated with increasing concentrations of ethanol, air-dried for 30 minutes, and then immediately subjected to microdissection using a PALM laser-microdissection microscope (Zeiss, Oberkochen, Germany) to collect the center nasal, center temporal, and OF regions of the OCs. Only those sections that showed an obvious presumptive vitreous cavity in the middle of the eye were used for sampling. It should be noted that pigmented RPE cells were deliberately excluded from the center nasal and center temporal OC samples, but presumptive RPE cells in the outer fold of the OF might be included in the OF samples (Fig. 1B). Tissues of each region from five embryos of the same litter were pooled together. Each region had three biological replicates (each from one separate litter; nine total samples corresponding to nine microarray chips). Total RNAs were isolated using TRIzol (Thermo Fisher Scientific, Waltham, MA, USA), linearly amplified and transcribed as cRNAs using a T7 transcription-based amplification strategy,²⁴ and hybridized to Affymetrix mouse genome 430 2.0 arrays (Thermo Fisher Scientific). All nine microarray samples were processed and hybridized in parallel. Robust multi-array analysis (RMA) was used to obtain gene expression data for each probe set,²⁵ a linear model approach was used to compare gene expression differences between groups,²⁶ and Benjamini-Yekutieli multitest correction method was applied to control the false discovery rate.²⁷ Adjusted $P \leq 0.05$ were considered significant. Gene Ontology (GO) term and Kyoto Encyclopedia of Genes and Genomes (KEGG) pathway enrichment analyses were performed using DAVID bioinformatics resources.²⁸ Microarray data have been deposited in GEO (GSE109501).

For quantitative RT-PCR verification of OF-specific genes, microdissection and RNA isolation were performed in the same way as for the microarray samples. Total RNAs were linearly amplified by being converted to double-stranded cDNAs using SuperScript Double-Stranded cDNA Synthesis Kit (Thermo Fisher Scientific) first, and then transcribed to amplified RNAs (aRNAs) using AmpliScribe T7 High Yield Transcription Kit (Epicentre, Madison, WI, USA). The primer used for the first-strand cDNA synthesis was as follows: 5'-TCTAGTCGACGGC CAGTGAATTGTAATACGACTCACTATAGGGCGT₂₁-3'.²⁹ Amplified RNAs were then reverse transcribed to cDNAs using random hexamers as the primers and SuperScript III (Thermo Fisher Scientific) as the enzyme. Quantitative PCR was then performed using individual gene-specific quantitative PCR (qPCR) primers and the SYBR green dye (Roche, Mannheim, Germany) detection method. *Gapdh* was used as the internal control, and the $\Delta\Delta C_t$ method was used to compare the gene expression levels between the OF and the central OC. Three pairs of the OF and central OC samples were used for each gene. The sequences for the primers used for quantitative RT-PCR are listed in Supplementary Table S1.

RNA In Situ Hybridization (ISH)

ISH probe-synthesizing plasmids were generated by cloning full-length or partial-length cDNAs of various genes into pGEMT-easy vectors (Promega, Madison, WI, USA). Primers used to RT-PCR amplify various genes are listed in Supplementary Table S1. Digoxigenin-labeled RNA probes were synthesized using either T7 or SP6 RNA polymerase (Promega). Mouse embryos were fixed in 4% formaldehyde overnight at 4°C, cryoprotected by soaking in 30% sucrose solution until sinking, embedded in OCT freezing medium, and frozen. The embryo OCT blocks were later sectioned using a cryostat microtome, mounted onto glass slides, and stored in a -20°C freezer. When performing ISH, frozen sections were thawed, rehydrated, postfixed with 4% formaldehyde for 10 minutes, digested with 1 µg/mL proteinase K for 5 minutes, and fixed again with 4% formaldehyde for 10 minutes. Treated slides

were then hybridized with specific probes in a humid chamber at 55°C to 65°C overnight. The next day, slides were washed and incubated with alkaline phosphatase-conjugated anti-digoxigenin antibody (Roche) at 4°C overnight. The third day, slides were washed and color-developed with NBT/BCIP reagents (Promega). Images were taken under a Zeiss Axio Observer Z1. Zebrafish embryo whole-mount ISH was performed as follows: Zebrafish embryos were fixed in 4% formaldehyde at 4°C overnight. Fixed embryos were digested with 1 µg/mL proteinase K for 5 to 10 minutes, postfixed for 5 minutes in 4% formaldehyde, and hybridized with digoxigenin-labeled RNA probes at 56°C to 65°C overnight. The next day, samples were washed and incubated with NTB-BCIP solution (Promega) for color development. Images were taken using the Leica stereomicroscope M205. To examine zebrafish whole-mount ISH signals on sections, after whole-mount ISH, fish embryos were fixed in 4% formaldehyde for 2 hours at room temperature, soaked in 30% sucrose until sinking, and then embedded in OCT freezing medium and frozen. Fish embryos embedded in OCT blocks were cut and mounted onto glass slides using a cryostat microtome, after which the slides were dehydrated with ethanol, covered with cover glass, and imaged using a Zeiss Axio Observer Z1.

Zebrafish Morpholino (MO), mRNA, and Plasmid Injection

The following MOs were purchased from Gene Tools (Philomath, OR, USA): *afap112*-MO1: CACTTTGTGCTTATC CATTCTCCAC (target translation initiation); *afap112*-MO2: GCTAAAGTAACTCACTGGTCTGGGA (target splicing between exon 4 and intron 4); *pax2a*-MO: ATATGGTGTCTCACCTA TAGTGTGT³⁰; and standard control MO (CCTCTTACCTCAGT TACAATTTATA). *afap112* full-length cDNA with a 3-nt silent mutation in the MO1 recognition sequence were cloned into pCS2 expression vectors; a mutant form of the *afap112*-cDNA-expressing plasmid was generated through site-directed mutagenesis to delete the A in the ATG-translation initiation codon. Capped mRNAs were synthesized using mMACHINE mMESSAGE transcription kit (Thermo Fisher Scientific). MOs, capped mRNAs, or plasmids were injected into one-cell stage embryos following a standard protocol.³¹

RESULTS

Region-Specific Transcriptomes of the Developing Retina

We used laser-assisted microdissection to collect different regions of the OCs of mouse embryos on embryonic day 11.5 (E11.5), the time point when the OF is closing, and then performed microarray analysis to obtain the transcriptomes of different OC regions. We collected cells that were within a five-cell diameter from the edge of the OF as the OF region, and we also collected OC cells in the center nasal retina (NR) and center temporal retina (TR) (Fig. 1B). Microarray data comparison analysis revealed that the NR and TR expressed almost identical transcriptomes. There were only 36 probe sets corresponding to 32 genes that showed significantly different expression levels between the NR and TR (Figs. 1C, 1D). Many known nasal-temporal retina polarity genes, such as *Foxg1*, *Foxd1*, *Hmx1*, *EfnA5*, *Epha5*, and *Tenm3*,^{32,33} exhibited NR- or TR-specific expression patterns, suggesting that our microarray analysis was reliable. Microarray comparison of the NR and TR also revealed several new nasal-temporal differentially expressed genes, including cell adhesion molecules (*Cdb9*, *Cdb11*, and *Sema5a*), transcription factors (*Sall1*, *Zfbx4*,

Onecut2, *Tfec*, and *Glis3*), and a noncoding RNA (*3110039M20Rik*), which may merit further study (Fig. 1D). In contrast, the OF transcriptome was dramatically different from the NR and TR transcriptomes. A total of 990 and 931 probe sets were significantly upregulated in the OF transcriptome relative to their levels in the NR or TR transcriptome, respectively, while 598 and 575 probe sets were significantly downregulated in the OF transcriptome relative to their levels in the NR or TR transcriptomes, respectively, suggesting a unique gene expression profile of the OF region (Fig. 1C). Most differentially expressed genes of the OF-NR/OFF-TR comparisons were common to both lists (Figs. 1E, 1F), which is consistent with the almost identical gene expression profiles between the NR and TR.

Gene Function Analysis of Differentially Expressed Genes Between the OF and Central OC

We performed GO term and KEGG pathway enrichment analyses to retrieve gene function profiles of the gene sets that were upregulated or depleted in the OF transcriptome. The analyses indicated that the OF upregulated gene set was enriched in cell-cell or cell-extracellular matrix interaction pathways (GO Biological Process [BP] terms: “cell adhesion” and “integrin-mediated signaling pathway”; GO Molecular Function [MF] terms: “integrin binding” and “extracellular matrix binding”; KEGG terms: “ECM-receptor interaction” and “focal adhesion,” Figs. 2A, 2C, 2E). The enrichment of these terms was consistent with the direct involvement of region cells in the OF closure morphogenesis process, which requires dynamic and active cell-cell and cell-extracellular matrix interactions. The OF upregulated gene set was enriched in GO BP terms such as “proteolysis involved in cellular protein catabolic process” and “positive regulation of tumor necrosis factor production” and KEGG pathways such as “lysosome,” “phagosome,” and “Fcγ R-mediated phagocytosis” (Figs. 2A, 2E), which may reflect active cell death and phagocytosis activity in the OF region.³⁴ The OF upregulated gene set was also enriched in GO MF terms such as “heparin binding” and “GTPase activator activity” (Fig. 2C), indicating that heparin binding proteins and GTPase activity are important for OF morphogenesis or function. The OF downregulated gene set was enriched in GO BP terms such as “cell cycle,” “cell division,” “mitotic nuclear division,” and “DNA replication” (Fig. 2B), which is consistent with the relatively slow proliferation activity of OF region cells.³⁵ Thus, transcriptome comparisons revealed that the OF region of the OC expresses a unique gene expression profile that corresponds to the specific morphogenesis requirement of OF region cells.

OF-Specific Genes

Among the list of OF highly enriched genes, there are many well-studied OF regulatory genes, including *Vax1*, *Vax2*, *Vax2os*,^{13,36,37} *Ntn1*,³⁸ *Smoc1*,³⁹ *Aldb1a3*,^{40,41} *Cyp1b1*,⁴² *Ptchd1*,⁴³ *Zfp503*,⁴⁴ *Laminins*,⁴⁵ *Bmpr1b*, *Bmp7*,^{46–48} and *Tenm3*.³³ However, no linkage has been drawn between most other OF-enriched genes and the OF. We focused on the top 45 genes that exhibited more than 5-fold enrichment in the OF transcriptome relative to the central OC transcriptomes (Fig. 3A) and performed RNA ISH of these genes on E11.5 mouse embryonic head cryosections to verify our microarray results and further characterize the OC expression patterns of these genes. ISH of approximately half of the genes did not result in any hybridization signals (data not shown), possibly due to differences in sample mRNA stability between the ISH preparation and the laser capture preparation or other technical factors. Using a set of independently microdissected

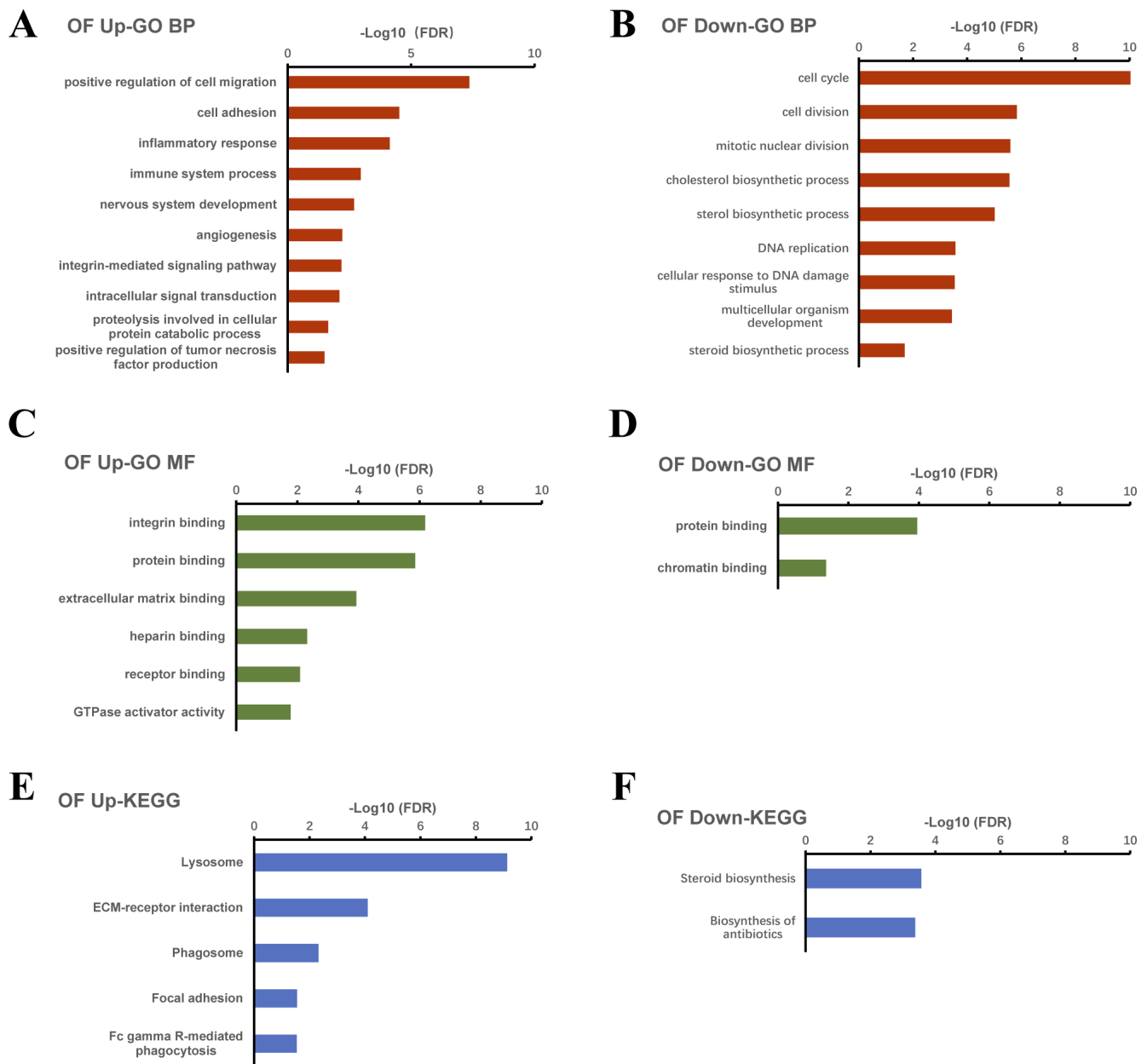


FIGURE 2. GO term and KEGG pathway enrichment analyses of DEGs between the OF and center OC. **(A)** Enriched GO Biological Process (BP) terms of OF upregulated genes. **(B)** Enriched GO BP terms of downregulated OF genes. **(C)** Enriched GO Molecular Function (MF) terms of upregulated OF genes. **(D)** Enriched GO MF terms of downregulated OF genes. **(E)** Enriched KEGG pathways of upregulated OF genes. **(F)** Enriched KEGG pathways of downregulated OF genes.

OF and central OC samples, we performed RNA linear amplification and then RT-qPCR experiments to compare the expression levels of these genes between the OF and the central OC. The results revealed that many of the genes that did not exhibit any ISH signals in the eye were indeed expressed at higher levels in the OF region than in the central OC (Supplementary Fig. S1). ISH of the genes that had demonstrated specific expression and/or critical functions in the OF, such as *Bmpr1b*,⁴⁸ *Ntn1*,³⁸ *Smoc1*,³⁹ *Aldb1a3*,⁴⁰ *Cyp1b1*,⁴² and *Vax2os*,³⁷ showed specific hybridization signals in the OF region as expected and served as ISH technical controls (Figs. 3M–R). There were several genes that exhibited sporadic dotted hybridization signals within the OC and in the vitreous fluid surrounding the OC, which resembled the cell distribution patterns of Iba-1⁺ microglial precursors (for *C1qc*,

Ctss, *C1qb*, *Laptm5*, *Mpeg1*, and *Cx3cr1*) or POM¹⁰ (for *Col3a1*), suggesting that these genes may be expressed in microglial precursors or POM (Figs. 3S–Y; Supplementary Fig. S2). The OF is a pathway for blood vessels and migrating POM cells to enter the eye; we dissected each OF region as a whole instead of dissecting the nasal and temporal OF regions separately (Fig. 1B), which might have introduced contamination by blood and POM cells into the OF samples and might have led to the inclusion of microglia/POM-specific genes in the OF-enriched gene set.

Most interestingly, ISH examination clearly demonstrated 11 new OF-specifically expressed genes, that is, *Afap112*, *Adamts16*, *Bmf*, *Slitrk1*, *Cp*, *Ror2*, *Tfec*, *Cplx3*, *Neto1*, *Sbtn1*, and *Flrt2* (Figs. 3B–L). *Afap112* is an adaptor protein that has been linked to tumorigenesis and airway repair.^{49,50} *Adamts16*

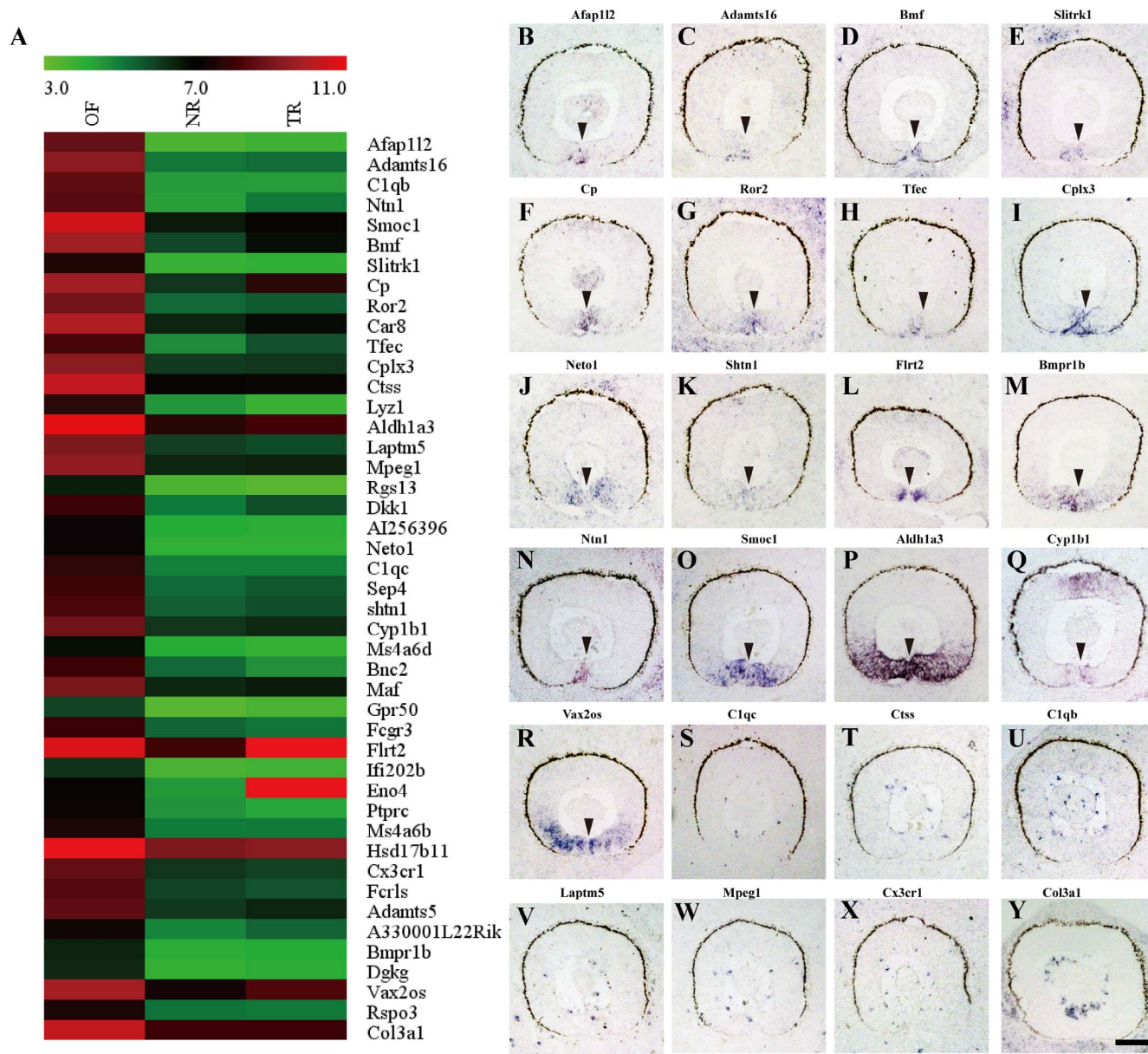


FIGURE 3. Tissue expression patterns of putative OF-specific genes in E11.5 mouse eyes. (A) Heatmap of OF-specific expressed genes that showed 5-fold enrichment in the OF region relative to the NR and TR. (B–L) Newly discovered OF-specific genes. (M–R) Known OF-specific genes. (S–Y) Mesenchymal/microglia genes. The scale bar in (Y) is 100 μm, and applies to all images in this figure.

is a member of a large family of metalloproteinases named a disintegrin-like and metalloproteinase with thrombospondin type 1 motif (ADAMTS), which has been linked to hypertension and genitourinary development.^{51–53} *Bmf* is a proapoptosis regulator⁵⁴ that might participate in the relatively active cell death activity in the OF region.³⁴ *Slitrk1*, *Neto1*, *Flrt2*, *Shtm1*, and *Cplx3* have functions in regulating neurite development in newly formed neurons,^{55–59} and their specific expression in the OF region might reflect the axon guidance function of OC cells at the OF edges. *Tfec* is in the same transcription factor family as *Mitf*, which is abundantly expressed in and controls the fate of RPE cells,⁶⁰ and the ISH signal of *Tfec* was specifically restricted to the very edge of the OF, which is more RPE-like³⁵ (in fact, *Mitf* was also enriched, but it was less prominent than *Tfec* in the OF transcriptome). *Cp* is a ferroxidase involved in iron metabolism.⁶¹ *Ror2* is a receptor tyrosine kinase involved in skeleton development regulation.⁶²

Further studies on how exactly these newly discovered OF-specific genes are involved in the development and function of the OF are merited.

afap112 Is Expressed at Zebrafish Closing OF

We chose zebrafish as the model system to perform functional tests due to conserved OC developmental processes between zebrafish and mammals, the faster development rate of zebrafish than that of mammals, and the availability of convenient gene manipulation tools for zebrafish. We selected *afap112*, the gene that exhibited the most highly enriched expression in the OF region in microarray transcriptome comparison analysis, for further functional analysis. We first performed ISH to examine the expression pattern of *afap112* in zebrafish. At 24 hpf, *afap112* was expressed strongly in the forebrain, but very weakly in the OC (Figs. 4A, 4B, 4B'). At 48

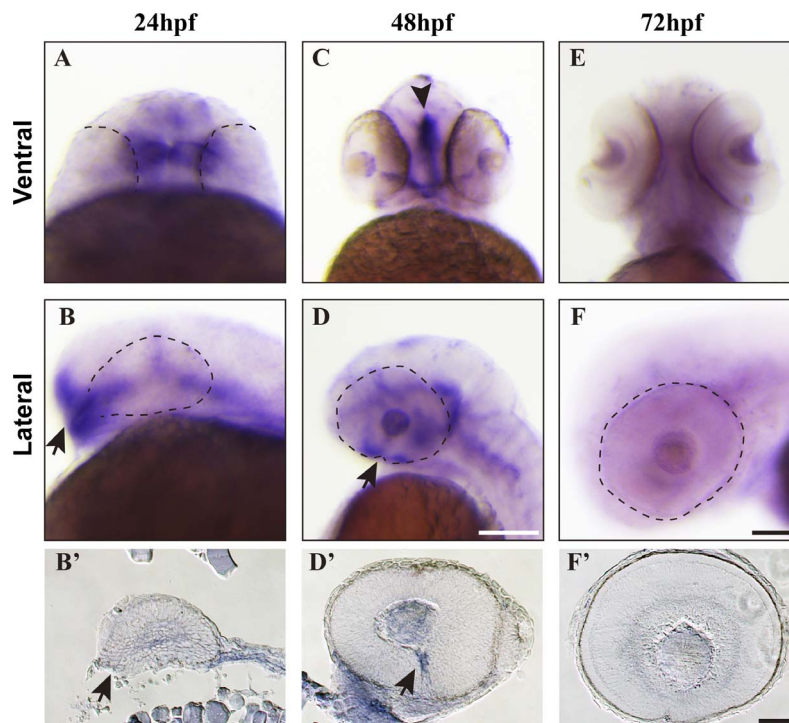


FIGURE 4. Zebrafish *afap112* is specifically expressed at the closing OF. Whole-mount RNA ISH of *afap112* in zebrafish embryos at 24 hpf (A, B, B'), 48 hpf (C, D, D'), and 72 hpf (E, F, F'). (A) A frontal view of a zebrafish head at 24 hpf. (C, E) Lateral views of zebrafish heads. (B, F) Ventral views of zebrafish heads. (B', F') Sagittal section images of zebrafish embryonic heads after *afap112* whole-mount ISH. Arrows in (B, B', D, D') point to the OF. The arrowhead in (C) points to the midline signal of *afap112*. Scale bars are all 100 μ m. The scale bar in (D) applies to (A–D); the scale bar in (F) applies to (E, F); and the scale bar in (F') applies to (B'–F').

hpf, *afap112* continued to be strongly expressed in the brain diencephalon midline (Fig. 4C). In addition, *afap112* was found to be strongly expressed in the OS and the OF region of the OC at this time point (Figs. 4C, 4D). In the OF region, *afap112* expression was restricted to the very edge of the closing OF, which can be clearly observed at the section level (Fig. 4D'). At 72 hpf, *afap112* expression disappeared from both the OC and the brain (Figs. 4E, 4E, 4F'). Thus, similar to the results in mice, zebrafish *afap112* is specifically expressed in the closing OF, suggesting that it might be involved in OF closure regulation.

afap112 Is Required for Proper Closure of the OF in Zebrafish

We synthesized two MOs, one targeting translation initiation (*afap112*-MO1) and the other one disrupting splicing between exon 4 and intron 4 (*afap112*-MO2, Fig. 5A), and performed one-cell zygote injection to study the function of *afap112* during zebrafish OF closure. The effectiveness of each MO was confirmed through either reporter knockdown assay (for MO1, Fig. 5B) or splicing variant RT-PCR (for MO2: Fig. 5C; Supplementary File S1). Since zebrafish OF closure normally occurs approximately 48 hpf and completes by 60 hpf¹⁸ (Cao MZ and Chen SY, unpublished observations, 2018), OF closure phenotype was examined at 72 hpf to exclude impact of developmental delay. At this time point, the ventral retina of the eyes of standard control MO-injected zebrafish had sealed tightly such that the eye was an integral sphere (Fig. 5D, the arrowhead points to the location where the previous OF would have been located). However, when *afap112* was knocked down by either MO1 or MO2, obvious clefts were observed on the ventral side of the eyes (Fig. 5D), demonstrating coloboma formation in these morphants. Coloboma penetrance exhibited dosage dependency for both MOs, reaching 80% at 4 ng for

MO1 and 6 ng for MO2 (Fig. 5E). Messenger RNA coinjection rescue experiments were performed to test whether the coloboma phenotype was caused specifically by *afap112* knockdown or by nonspecific/off-target effects of MO injection. We synthesized capped *afap112* mRNA containing 3-nt silent mutations to avoid MO1 targeting. Indeed, coinjecting MO1 or MO2 with *afap112*-mRNA rescued coloboma phenotype to 20%, whereas coinjection with a mutant form of *afap112*-mRNA in which the T in ATG-translation initiation codon was deleted did not rescue the coloboma phenotype (Fig. 5F), demonstrating the specificity of both MOs against *afap112*. Thus, the MO knockdown experiments demonstrated that *afap112* is required for proper closure of the OF in zebrafish.

afap112 Regulates OF Closure by Regulating Expression of *pax2a*

We used ISH to examine the expression of several known important OF closure regulatory genes to investigate how *afap112* regulates OF closure. OF development closely relates to ventral retina development^{11–13}; we therefore examined the expression of *tbx5a* and *aldh1a2*, two dorsal retina markers, and *vax2* and *aldh1a3*, two ventral retina markers, but no expression change was observed in *afap112*-morphant eyes (Supplementary Figs. S3A–H), suggesting that dorsal-ventral retinal fates were properly established. The POM plays important regulatory roles in OF closure^{17,20}; we therefore examined the expression of *foxc1a*, a marker and important regulator of POM cells. The result showed that *foxc1a*-expressing POM cells were normally developed in *afap112*-morphant eyes (Supplementary Figs. S3I, S3J). *Pax2* is one of the most important regulatory transcription factors controlling the proximal fates of the retina primordium, including the OS

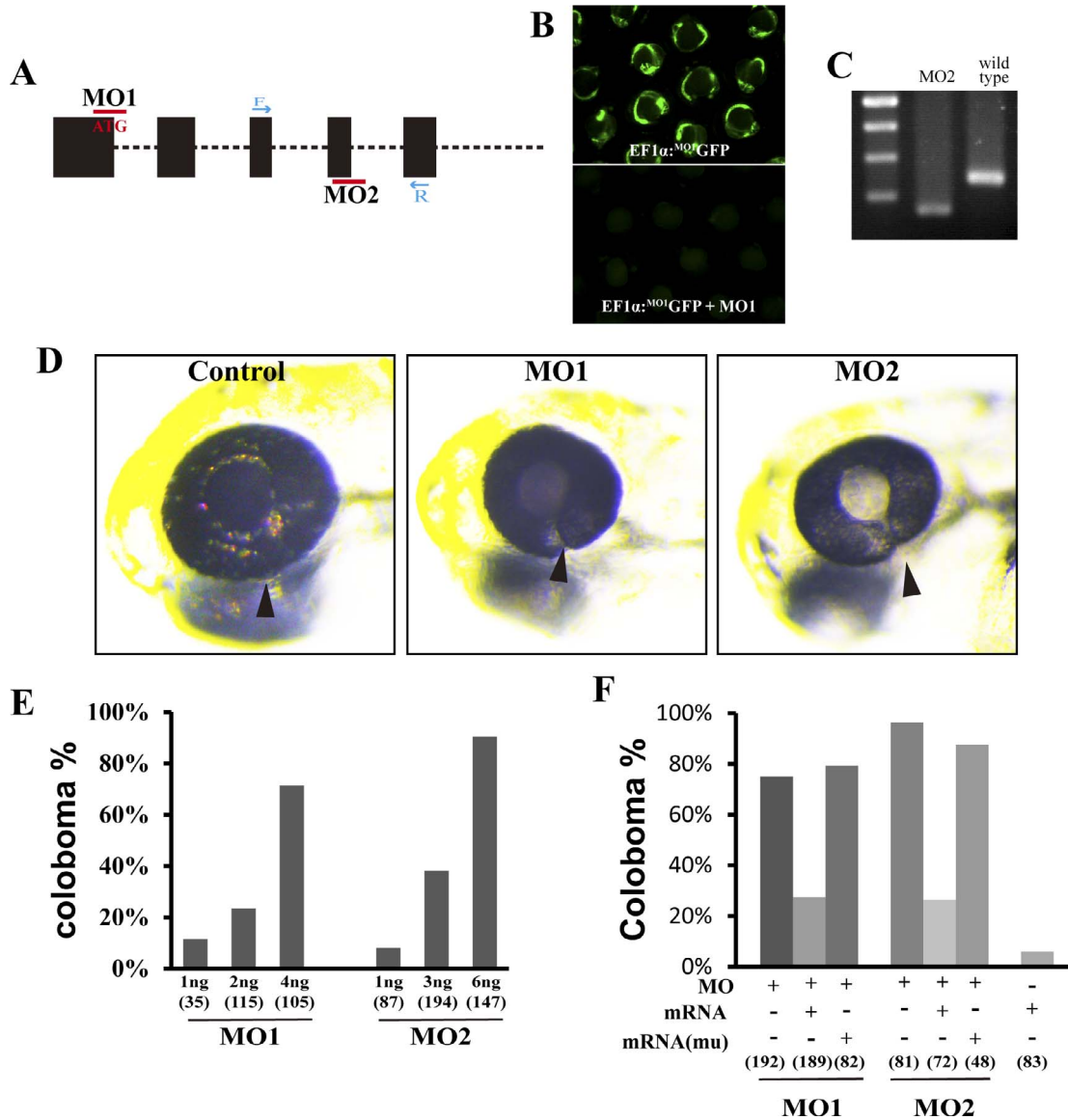


FIGURE 5. *afap112* is required for proper closure of the OF in zebrafish. (A) The diagram of partial zebrafish *afap112* gene structure illustrates the targeting positions of MO1 and MO2 and the locations of primers for splicing variant RT-PCR. (B) MO1 knockdown efficacy reporter assay showing that coinjecting MO1 with the reporter plasmid blocked GFP expression. (C) MO2 knockdown efficiency RT-PCR assay showing that MO2 knockdown resulted in shorter amplicons lacking exon 4. (D) Eye images of control and *afap112* morphants. Arrowheads point to the OF (E) Quantification of percentage of coloboma incidences in *afap112*-morphant zebrafish shows that the penetrance of both *afap112* MOs exhibited dosage dependency. (F) Quantification of incidences of coloboma phenotype of *afap112* mRNA rescue experiments. mRNA (mu): mutant form of *afap112* mRNA. Numbers at the bottom of each column in (E, F) denote the number of zebrafish used in each experimental group.

and the OF,⁶⁵ and mutation of *Pax2* in both mice and zebrafish causes coloboma formation.^{15,64} Interestingly, ISH examination of *pax2a* expression showed that it was dramatically upregulated in the ventral OC of *afap112*-morphant eyes, expanding from the edges of the OF region into the OC at 36 hpf (Figs. 6A–D). To examine whether there is reciprocal regulation between *afap112* and *pax2a*, we measured *afap112* expression in the eyes of *pax2a* morphants. The qPCR result revealed that *afap112* was expressed at a similar level in the eyes of *pax2a* morphants as in wild-type control fish (Fig. 6G). In addition, overexpressing *afap112* did not repress the expression of *pax2a* in the eye (Figs. 6E, 6F). These results demonstrate that there is no reciprocal regulation between *afap112* and *pax2a*. It has been shown in chicks that overexpression of *Pax2* phenocopies loss of *Pax2* to cause coloboma formation⁶⁵; we therefore wanted to test whether

coloboma formation in *afap112* morphants was caused by upregulated *pax2a* expression. For this purpose, we knocked down *pax2a* in *afap112* morphants by coinjecting *afap112*-MO with *pax2a*-MO. As reported, knocking down *pax2a* alone caused coloboma formation⁶⁴ (Fig. 6H; Supplementary Fig. S4C); however, coinjecting *afap112*-MO and *pax2a*-MO prominently rescued the coloboma phenotype in both morphants (Fig. 6H; Supplementary Fig. S4D), demonstrating that *pax2a* upregulation was a major cause of coloboma formation in *afap112*-morphant zebrafish.

DISCUSSION

In this study, we characterized the unique transcriptome of OC tissue in the OF region, providing a valuable foundation for

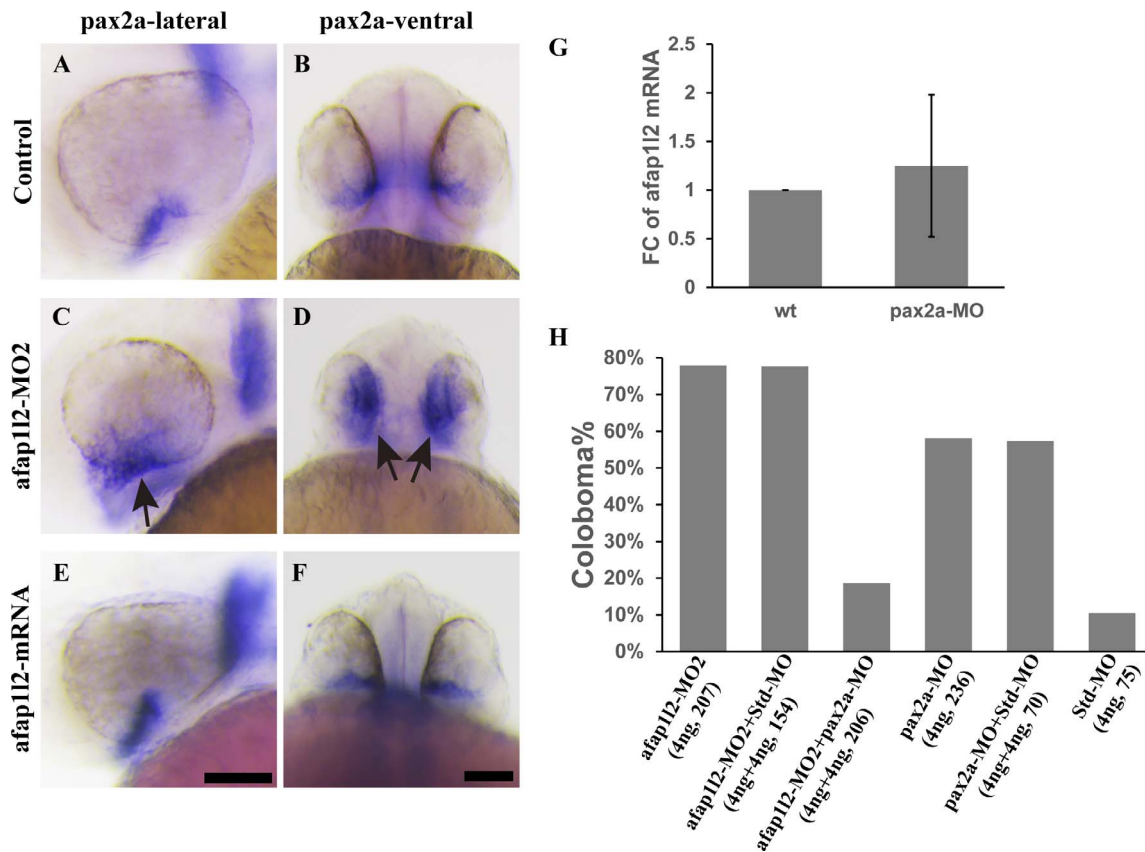


FIGURE 6. *afap112* controls OF closure by regulating *pax2a* expression. (A–F) ISH of *pax2a* in the eyes of control, *afap112*-morphant, and *afap112*-overexpressing zebrafish at 36 hpf. (A, B) Lateral views; (C, D) ventral views. (G) qPCR comparison of *afap112* expression levels in the eyes of wild-type and *pax2a*-morphant zebrafish. FC: fold change. (H) Quantification of incidences of coloboma phenotype of *afap112*-MO and *pax2a*-MO coinjection. Numbers in parentheses denote dosage of the morpholinos used and the number of zebrafish injected. The scale bars in (E, F) are both 100 μ m, and they apply to (A, C, E) and to (B, D, F), respectively.

future OF developmental and functional mechanism studies. The study also revealed the essential role of a newly discovered OF-specific gene, *Afap112*, during OF closure, further suggesting the importance of OF-specific genes for OF development and function.

Human ophthalmic genetic studies and animal model studies have linked many genes with coloboma formation and thus OF closure. However, the genetic etiology of most coloboma cases remains unsolved, illustrating the complexity of the regulatory mechanisms governing the OF closure process.¹ Many of the known coloboma causative genes are expressed in the OF region, for example, *Pax2*, *Vax1*, and *Vax2*. Since the retinal progenitor cells in the OF region are the cells that directly participate in the OF closure process, they may express a unique transcriptome to support their OF closure task. Thus, characterizing the unique OF transcriptome may help us find new OF closure regulatory genes and pathways. Indeed, in dramatic contrast to central OC regions, which exhibited almost identical expression profiles, the OF region showed a distinct expression profile: Over a thousand genes were differentially expressed in the OF region relative to central OCs, demonstrating the unique gene expression profile of the OF region. We were particularly interested in the group of genes specifically enriched in the OF transcriptome because this group of genes might contain important OF closure regulatory genes. Indeed, many known OF regulatory genes are among the OF-enriched genes list. For example, *Vax1*, *Vax2*, *Smoc1*, *Zfp503*, and regulators of cellular processes essential for OF morphogenesis, such as cell-cell and cell-extracellular

matrix interactions, are all enriched in the list, suggesting the reliability and usefulness of our OF-specific transcriptome analysis. In addition to known OF regulatory genes, the OF-enriched gene list contains many genes of various pathways whose functions have not been linked to OF development and physiology that may merit further investigation. Indeed, in this study, we found that *Afap112*, the gene most highly enriched in the OF transcriptome in microarray comparisons, plays important roles in regulating OF closure. In addition, the OF also has an important function in guiding the projection of axons of newly generated retinal ganglion cells. In addition to the known retinal ganglion cell guidance molecules *Ntn1* and *Tenm3*, the molecular functions of some newly discovered OF-specific genes, such as *Slitrk1*, *Cplx3*, *Sbtn1*, *Flrt2*, and *Flrt1*, suggest that these genes may be involved in the axon guidance function of the OF. One caveat that should be noted is that slightly different dissection ranges were used for the central OC samples and the OF samples. We deliberately excluded pigmented RPE cells from the NR and TR samples, but a few pigmented RPE cells and presumptive RPE cells in the outer fold of the OF might be included in our OF samples. The enrichment of *Mitf*, a transcription factor known to promote an RPE cell fate, suggests that some RPE/presumptive RPE cells were likely included in our OF samples. A secondary analysis comparing our OF-specific gene list to a list of RPE “signature” genes⁶⁶ found only 15 (*Aldb1a3*, *Ankrd12*, *Crx*, *Dzip1*, *Itgav*, *Itm2b*, *Lamp2*, *Lgals8*, *Mbnl2*, *Pknox2*, *Ptprg*, *Rab38*, *Sema3c*, *Sorbs2*, *Trpm1*) out of 154 RPE “signature” genes in our OF enriched gene list (861 genes), while many well-

known RPE signature genes, such as *Dct* and *Tyrp1*, were not enriched in our OF samples. This fact, in conjunction with our attempts to deliberately exclude pigmented cells from the OF dissection, suggests that these genes represent the inclusion of nonpigmented presumptive RPE cells prior to their being fully differentiated.

So far, only one transcriptome-wide gene expression analysis has been conducted on OC tissues in the OF region. Similar to our study, Brown et al.⁴⁴ used laser-assisted microdissection to specifically dissect cells in the OF region and used microarrays to obtain the transcriptomes of OF region cells. Brown et al. found 222 genes whose expression exhibited dynamic changes during OF development by comparing the transcriptomes of OF region cells at the open (E10.5), closing (E11.5), and fused (E12.5) stages. Their study illustrated the dynamic adjustment of gene expression in the OF to accommodate specific demands of the closing process, but it might have missed many important OF closure regulatory genes that are constantly expressed in the region. Comparing the list of OF-specific genes from this study and the list of 222 dynamically expressed OF genes from Brown et al., there were 27 overlapping genes in the two lists: *Cplx3*, *Ascl1*, *Zfp503*, *Cyp1b1*, *Mpeg1*, *Bmpr1b*, *A330001L22Rik*, *Dlc1*, *Meg3*, *Col23a1*, *Gnai1*, *Chst11*, *Tmem176b*, *Eno4*, *Rgs16*, *4833424015Rik*, *Smoc1*, *Lamb1*, *Camk4*, *Prpf4b*, *Hist1b1c*, *Soat1*, *Pdlim5*, *Tmem191c*, *Sox6*, *Pon2*, and *Pea15a*. This indicated that the expression of some OF-specific genes is also dynamically regulated during OF development. Among these 27 genes, *Zfp503*,⁴⁴ *Cyp1b1*,⁴² *Bmpr1b*,⁴⁷ *Smoc1*,³⁹ and *Lamb1*⁴⁵ have been demonstrated to be essential for proper closure of the OF. How these OF-specific genes are dynamically regulated and whether their dynamic expression is important for proper OF closure is unclear. Our study and that of Brown et al. may complement each other, providing a comprehensive gene expression profile of the OF, which would be a valuable basis for further OF regulation mechanism dissections.

Afap112 is a member of AFAP (actin filament associated protein) family but lacks the C-terminal actin binding domain. *Afap112* has multiple functional domains and has been shown to interact with various proteins and lipids to mediate signaling transduction and regulate cell proliferation, migration, and survival.⁵⁰ *Afap112* stood out as the most highly enriched gene in the OF transcriptome in our microarray comparison analysis, and its OF-specific expression was subsequently confirmed by ISH examination. No previous study had indicated the function of *Afap112* in tissue morphogenesis, including in the eye. This study demonstrated that *afap112* is required for proper OF closure, illustrating the importance of OF-specific genes for its development. We found that *pax2a* was upregulated in *afap112*-morphant eyes in the OF region. *Pax2* is specifically expressed in the OF region and is one of the most important regulators of OF development.¹⁵ It has been demonstrated that *Pax2* dosage needs to be tightly controlled to ensure proper OF closure^{15,65,67}; thus, upregulated *pax2a* expression in *afap112* morphants could be the major cause of coloboma formation. Indeed, knocking down *pax2a* rescued the coloboma phenotype in *afap112*-knockdown zebrafish, demonstrating that *pax2a* is a downstream target of *afap112* during OF closure. Studies using cultured cells have shown that *Afap112* is localized in the cytoplasm as an adaptor protein and interacts with multiple signaling pathway components, such as the Src kinase and PI3K/Akt kinase signaling pathways, to control gene expression.⁵⁰ Since *afap112* is an OF-specific gene and its expression domain overlaps with or is even more restricted than that of *pax2a*, we speculate that *afap112* restricts the activity of the

signaling pathway(s) that promotes the expression of *pax2a* in the proximal region of the eye primordium, thus restricting the expression of *pax2a* from expanding into the neural retina. *shha* secreted from the body midline promotes the proximal eye primordial fates and *pax2a* expression.¹⁶ However, SHH signaling activity remained relatively unchanged in *afap112* morphants (Supplementary Fig. S5). Thus, *afap112* might control the expression of *pax2a* in the OF region through other signaling pathway(s) or factors (such as *pax6a*, a transcription factor that represses the expression of *pax2a*), which needs further investigation.

Acknowledgments

The authors thank Mengqing Xiang, PhD, for critical reading of the manuscript, the zebrafish facility and Xiaoling Guo at Sun Yat-sen Medical School for preparing zebrafish embryos and providing technical support, and Qingjiong Zhang, PhD, for providing zebrafish maintenance equipment.

Supported by the National Natural Science Foundation of China (81371057), Guangzhou Science Technology and Innovation Commission (201504010030), Guangdong Provincial Department of Science and Technology (2015B020225003), and the Ministry of Science and Technology of China 973 program (2015CB964600).

Disclosure: **M. Cao**, None; **J. Ouyang**, None; **H. Liang**, None; **J. Guo**, None; **S. Lin**, None; **S. Yang**, None; **T. Xie**, None; **S. Chen**, None

References

1. Chang L, Blain D, Bertuzzi S, Brooks BP. Uveal coloboma: clinical and basic science update. *Curr Opin Ophthalmol*. 2006;17:447-470.
2. Gregory-Evans CY, Williams MJ, Halford S, Gregory-Evans K. Ocular coloboma: a reassessment in the age of molecular neuroscience. *J Med Genet*. 2004;41:881-891.
3. Hornby SJ, Ward SJ, Gilbert CE, et al. Environmental risk factors in congenital malformations of the eye. *Ann Trop Paediatr*. 2002;22:67-77.
4. Kelberman D, Islam L, Lakowski J, et al. Mutation of SALL2 causes recessive ocular coloboma in humans and mice. *Hum Mol Genet*. 2014;23:2511-2526.
5. Wang L, He F, Bu J, et al. ABCB6 mutations cause ocular coloboma. *Am J Hum Genet*. 2012;90:40-48.
6. Vissers LE, van Ravenswaaij CM, Admiraal R, et al. Mutations in a new member of the chromodomain gene family cause CHARGE syndrome. *Nat Genet*. 2004;36:955-957.
7. Bardakjian T, Weiss A, Schneider A. Microphthalmia/Anophthalmia/Coloboma Spectrum. In: Adam MP, Ardinger HH, Pagon RA, eds. *GeneReviews*[®] [Internet]. Seattle, WA: University of Washington, Seattle; 1993-2018.
8. Chow RL, Lang RA. Early eye development in vertebrates. *Annu Rev Cell Dev Biol*. 2001;17:255-296.
9. Adler R, Canto-Soler MV. Molecular mechanisms of optic vesicle development: complexities, ambiguities and controversies. *Dev Biol*. 2007;305:1-13.
10. Gage PJ, Rhoades W, Prucka SK, Hjalt T. Fate maps of neural crest and mesoderm in the mammalian eye. *Invest Ophthalmol Vis Sci*. 2005;46:4200-4208.
11. Uemonsa T, Sakagami K, Yasuda K, Araki M. Development of dorsal-ventral polarity in the optic vesicle and its presumptive role in eye morphogenesis as shown by embryonic transplantation and in ovo explant culturing. *Dev Biol*. 2002;248:319-330.
12. Barbieri AM, Broccoli V, Bovolenta P, et al. *Vax2* inactivation in mouse determines alteration of the eye dorsal-ventral axis,

- misrouting of the optic fibres and eye coloboma. *Development*. 2002;129:805–813.
13. Mui SH, Kim JW, Lemke G, Bertuzzi S. Vax genes ventralize the embryonic eye. *Genes Dev*. 2005;19:1249–1259.
 14. Take-uchi M, Clarke JD, Wilson SW. Hedgehog signalling maintains the optic stalk-retinal interface through the regulation of Vax gene activity. *Development*. 2003;130:955–968.
 15. Torres M, Gomez-Pardo E, Gruss P. Pax2 contributes to inner ear patterning and optic nerve trajectory. *Development*. 1996;122:3381–3391.
 16. Macdonald R, Barth KA, Xu Q, et al. Midline signalling is required for Pax gene regulation and patterning of the eyes. *Development*. 1995;121:3267–3278.
 17. Lupo G, Gestri G, O'Brien M, et al. Retinoic acid receptor signaling regulates choroid fissure closure through independent mechanisms in the ventral optic cup and periocular mesenchyme. *Proc Natl Acad Sci U S A*. 2011;108:8698–8703.
 18. James A, Lee C, Williams AM, et al. The hyaloid vasculature facilitates basement membrane breakdown during choroid fissure closure in the zebrafish eye. *Dev Biol*. 2016;419:262–272.
 19. McMahon C, Gestri G, Wilson SW, Link BA. Lmx1b is essential for survival of periocular mesenchymal cells and influences Fgf-mediated retinal patterning in zebrafish. *Dev Biol*. 2009;332:287–298.
 20. Bajpai R, Chen DA, Rada-Iglesias A, et al. CHD7 cooperates with PBAF to control multipotent neural crest formation. *Nature*. 2010;463:958–962.
 21. Kim TH, Goodman J, Anderson KV, Niswander L. Phacr4 regulates neural tube and optic fissure closure by controlling PP1-, Rb-, and E2F1-regulated cell-cycle progression. *Dev Cell*. 2007;13:87–102.
 22. Shi Y, Tu Y, Mecham RP, Bassnett S. Ocular phenotype of Fbn2-null mice. *Invest Ophthalmol Vis Sci*. 2013;54:7163–7173.
 23. Chen S, Lewis B, Moran A, Xie T. Cadherin-mediated cell adhesion is critical for the closing of the mouse optic fissure. *PLoS One*. 2012;7:e51705.
 24. Van Gelder RN, von Zastrow ME, Yool A, et al. Amplified RNA synthesized from limited quantities of heterogeneous cDNA. *Proc Natl Acad Sci U S A*. 1990;87:1663–1667.
 25. Irizarry RA, Bolstad BM, Collin F, et al. Summaries of Affymetrix GeneChip probe level data. *Nucleic Acids Res*. 2003;31:e15.
 26. Smyth GK. Linear models and empirical bayes methods for assessing differential expression in microarray experiments. *Stat Appl Genet Mol Biol*. 2004;3:Article 3.
 27. Benjamini Y, Yekutieli D. The control of the false discovery rate in multiple testing under dependency. *Ann Stat*. 2001;29:1165–1188.
 28. Huang DW, Sherman BT, Lempicki RA. Systematic and integrative analysis of large gene lists using DAVID bioinformatics resources. *Nat Protoc*. 2009;4:44–57.
 29. Luo L, Salunga RC, Guo H, et al. Gene expression profiles of laser-captured adjacent neuronal subtypes. *Nat Med*. 1999;5:117–122.
 30. McCarroll MN, Lewis ZR, Culbertson MD, et al. Graded levels of Pax2a and Pax8 regulate cell differentiation during sensory placode formation. *Development*. 2012;139:2740–2750.
 31. Moulton JD, Yan YL. Using Morpholinos to control gene expression. *Curr Protoc Mol Biol*. 2008; Chapter 26:Unit 26.8.
 32. McLaughlin T, Hindges R, O'Leary DD. Regulation of axial patterning of the retina and its topographic mapping in the brain. *Curr Opin Neurobiol*. 2003;13:57–69.
 33. Leamey CA, Merlin S, Lattouf P, et al. Ten_m3 regulates eye-specific patterning in the mammalian visual pathway and is required for binocular vision. *PLoS Biol*. 2007;5:e241.
 34. Hero I. Optic fissure closure in the normal cinnamon mouse. An ultrastructural study. *Invest Ophthalmol Vis Sci*. 1990;31:197–216.
 35. Chen S, Li H, Gaudenz K, et al. Defective FGF signaling causes coloboma formation and disrupts retinal neurogenesis. *Cell Res*. 2013;23:254–273.
 36. Bertuzzi S, Hindges R, Mui SH, et al. The homeodomain protein vax1 is required for axon guidance and major tract formation in the developing forebrain. *Genes Dev*. 1999;13:3092–3105.
 37. Meola N, Pizzo M, Alfano G, et al. The long noncoding RNA Vax2os1 controls the cell cycle progression of photoreceptor progenitors in the mouse retina. *RNA*. 2012;18:111–123.
 38. Deiner MS, Kennedy TE, Fazeli A, et al. Netrin-1 and DCC mediate axon guidance locally at the optic disc: loss of function leads to optic nerve hypoplasia. *Neuron*. 1997;19:575–589.
 39. Okada I, Hamanoue H, Terada K, et al. SMOC1 is essential for ocular and limb development in humans and mice. *Am J Hum Genet*. 2011;88:30–41.
 40. Dupe V, Matt N, Garnier JM, et al. A newborn lethal defect due to inactivation of retinaldehyde dehydrogenase type 3 is prevented by maternal retinoic acid treatment. *Proc Natl Acad Sci U S A*. 2003;100:14036–14041.
 41. Molotkov A, Molotkova N, Duester G. Retinoic acid guides eye morphogenetic movements via paracrine signaling but is unnecessary for retinal dorsoventral patterning. *Development*. 2006;133:1901–1910.
 42. Williams AL, Eason J, Chawla B, Bohnsack BL. Cyp1b1 regulates ocular fissure closure through a retinoic acid-independent pathway. *Invest Ophthalmol Vis Sci*. 2017;58:1084–1097.
 43. Lee J, Willer JR, Willer GB, et al. Zebrafish blowout provides genetic evidence for Patched1-mediated negative regulation of Hedgehog signaling within the proximal optic vesicle of the vertebrate eye. *Dev Biol*. 2008;319:10–22.
 44. Brown JD, Dutta S, Bharti K, et al. Expression profiling during ocular development identifies 2 Nlz genes with a critical role in optic fissure closure. *Proc Natl Acad Sci U S A*. 2009;106:1462–1467.
 45. Lee J, Gross JM. Laminin beta1 and gamma1 containing laminins are essential for basement membrane integrity in the zebrafish eye. *Invest Ophthalmol Vis Sci*. 2007;48:2483–2490.
 46. Morcillo J, Martinez-Morales JR, Trousse F, et al. Proper patterning of the optic fissure requires the sequential activity of BMP7 and SHH. *Development*. 2006;133:3179–3190.
 47. Murali D, Yoshikawa S, Corrigan RR, et al. Distinct developmental programs require different levels of Bmp signaling during mouse retinal development. *Development*. 2005;132:913–923.
 48. Furuta Y, Hogan BL. BMP4 is essential for lens induction in the mouse embryo. *Genes Dev*. 1998;12:3764–3775.
 49. Zhao J, Wang Y, Wakeham A, et al. XB130 deficiency affects tracheal epithelial differentiation during airway repair. *PLoS One*. 2014;9:e108952.
 50. Bai XH, Cho HR, Moodley S, Liu M. XB130—a novel adaptor protein: gene, function, and roles in tumorigenesis. *Scientifica (Catro)*. 2014;2014:903014.
 51. Jacobi CL, Rudigier LJ, Scholz H, Kirschner KM. Transcriptional regulation by the Wilms tumor protein, Wt1, suggests a role of the metalloproteinase Adamts16 in murine genitourinary development. *J Biol Chem*. 2013;288:18811–18824.

52. Joe B, Saad Y, Dhindaw S, et al. Positional identification of variants of Adamts16 linked to inherited hypertension. *Hum Mol Genet.* 2009;18:2825–2838.
53. Apte SS. A disintegrin-like and metalloprotease (reprolysin-type) with thrombospondin type 1 motif (ADAMTS) superfamily: functions and mechanisms. *J Biol Chem.* 2009;284:31493–31497.
54. Labi V, Woess C, Tuzlak S, et al. Deregulated cell death and lymphocyte homeostasis cause premature lethality in mice lacking the BH3-only proteins Bim and Bmf. *Blood.* 2014;123:2652–2662.
55. Aruga J, Mikoshiba K. Identification and characterization of Slitrk, a novel neuronal transmembrane protein family controlling neurite outgrowth. *Mol Cell Neurosci.* 2003;24:117–129.
56. Yamagishi S, Hampel F, Hata K, et al. FLRT2 and FLRT3 act as repulsive guidance cues for Unc5-positive neurons. *EMBO J.* 2011;30:2920–2933.
57. Shimada T, Toriyama M, Uemura K, et al. Shootin1 interacts with actin retrograde flow and L1-CAM to promote axon outgrowth. *J Cell Biol.* 2008;181:817–829.
58. Reim K, Regus-Leidig H, Ammermuller J, et al. Aberrant function and structure of retinal ribbon synapses in the absence of complexin 3 and complexin 4. *J Cell Sci.* 2009;122:1352–1361.
59. Ng D, Pitcher GM, Szilard RK, et al. Neto1 is a novel CUB-domain NMDA receptor-interacting protein required for synaptic plasticity and learning. *PLoS Biol.* 2009;7:e41.
60. Bharti K, Gasper M, Ou J, et al. A regulatory loop involving PAX6, MITE, and WNT signaling controls retinal pigment epithelium development. *PLoS Genet.* 2012;8:e1002757.
61. Texel SJ, Zhang J, Camandola S, et al. Ceruloplasmin deficiency reduces levels of iron and BDNF in the cortex and striatum of young mice and increases their vulnerability to stroke. *PLoS One.* 2011;6:e25077.
62. DeChiara TM, Kimble RB, Poueymirou WT, et al. Ror2, encoding a receptor-like tyrosine kinase, is required for cartilage and growth plate development. *Nat Genet.* 2000;24:271–274.
63. Schwarz M, Cecconi F, Bernier G, et al. Spatial specification of mammalian eye territories by reciprocal transcriptional repression of Pax2 and Pax6. *Development.* 2000;127:4325–4334.
64. Macdonald R, Scholes J, Strahle U, et al. The Pax protein Noi is required for commissural axon pathway formation in the rostral forebrain. *Development.* 1997;124:2397–2408.
65. Sehgal R, Karcavich R, Carlson S, Belecky-Adams TL. Ectopic Pax2 expression in chick ventral optic cup phenocopies loss of Pax2 expression. *Dev Biol.* 2008;319:23–33.
66. Strunnikova NV, Maminishkis A, Barb JJ, et al. Transcriptome analysis and molecular signature of human retinal pigment epithelium. *Hum Mol Genet.* 2010;19:2468–2486.
67. Heisenberg CP, Brennan C, Wilson SW. Zebrafish aussicht mutant embryos exhibit widespread overexpression of ace (fgf8) and coincident defects in CNS development. *Development.* 1999;126:2129–2140.